TaPCNA plays a role in programmed cell death after UV-B exposure in wheat (*Triticum aestivum*)

Meiting Du[A], *Ying Zhang*[A], *Huize Chen* (iD)[A,B] *and Rong Han*[A,B]

[A]Higher Education Key Laboratory of Plant Molecular and Environment Stress Response
 (Shanxi Normal University) in Shanxi Province, Linfen City, Shanxi Province, China.
[B]Corresponding authors. Emails: chenhuize@hotmail.com; snuchen@snu.ac.kr

Abstract. Ultraviolet (UV)-B is a component of sunlight and shows a significant effect on DNA damage, which can be regulated by proliferating cell nuclear antigen (PCNA). The role of TaPCNA in wheat (*Triticum aestivum* L.) programmed cell death (PCD) under UV-B has not been investigated previously. Here, we explored the function of TaPCNA in wheat exposed to UV-B utilising Barley Stripe Mosaic Virus–virus-induced gene silencing (VIGS). The results showed that the expression of *TaPCNA* was downregulated, and curly wheat leaves with several spots were determined by VIGS. The growth rate and mesophyll cell length were significantly inhibited after *TaPCNA* was silenced. The activity of superoxide dismutase and the contents of soluble sugar and soluble protein decreased, whereas the activities of peroxidase and catalase and malondialdehyde content increased in *TaPCNA*-silenced and UV-B treatment groups. DNA laddering and propidium iodide staining results showed that DNA fragments and micronucleus accumulated after TaPCNA silencing with or without UV-B. Thus, TaPCNA participates in plant growth and DNA damage and PCD under UV-B. This study suggests an idea for the exploration of the function of certain genes in such complex wheat genomes and offers a theoretical basis to improve wheat agronomic traits.

Keywords: programmed cell death, gene silencing, wheat, UV-B radiation, proliferating cell nuclear antigen, *Triticum aestivum* L.

Introduction

Proliferating cell nuclear antigen (PCNA) is an evolutionally conserved protein found in all eukaryotic species and archaea. PCNA was initially identified as a co-factor for DNA polymerase δ, which is needed for DNA synthesis during its replication (Kelman 1997). More than 30 years ago, PCNA was identified as an antigen of autoimmune disease in the serum of patients with systemic lupus erythematosus. Subsequent studies showed that the expression level of PCNA is associated with tumour proliferation or transformation (Paunesku *et al*. 2001). In addition to DNA replication, PCNA functions in other important cellular processes, such as chromatin assembly, DNA damage repair, and sister chromatid aggregation (Maga and Hübscher 2003), and has the same function as cyclin (Strzalka and Ziemienowicz 2011).

Given that plants are continuously exposed to living factors (endogenous and environmental), hereditary material can be damaged in various ways. The accumulation of spontaneous or induced mutations in large numbers of divided cells may disrupt the normal metabolism of the whole plant (Chen and Gao 2015). Endogenous mutagens mainly include reactive free radicals, such as hydroxyl radicals, nitric oxide, and superoxide anions, whereas environmental mutagens mainly comprise environmental mutagens, including ultraviolet radiation, ionising radiation, and chemical substances. The biological effects of such mutagens depend on the type of DNA damage, which results in uncontrolled cell proliferation or death (Mailand *et al*. 2013). Meanwhile, the DNA repair systems include PCNA proteins, which stabilise the inheritance of undamaged genetic information (Essers *et al*. 2005).

As the earliest cultivated and widely distributed crop, wheat (*Triticum aestivum* L.) provides basic food for people all over the world (Shewry 2009; Kuhlmann and Müller 2010). Ultraviolet (UV)-B is a component of sunlight and shows a critical effect on crop plants (Yin and Ulm 2017), especially on wheat seedlings (Lizana *et al*. 2009). Elevated UV-B radiation-induced DNA damage (Ries *et al*. 2000; Nawkar *et al*. 2013), and reduced genome stability in plants reduce the rates of cell division and elongation in the primary leaf of wheat (Hopkins *et al*. 2002). All these key processes can be affected by the PCNA. However, the function of TaPCNA under UV-B has not been investigated previously. Here, we generated Barley Stripe Mosaic Virus (BSMV):*TaPCNA* vectors for the targeted silencing of wheat by using BSMV-virus-induced gene silencing (VIGS). The results showed that TaPCNA is crucial in DNA damage and programmed cell death (PCD) of wheat under UV-B, providing insights into the

plant response to UV-B and supplying a viable way to explore gene functions in wheat.

Materials and methods

Plant material and culture conditions

Wheat (*Triticum aestivum* L.) cv. Yimai 325 was donated by Shanxi Wheat Research Institute was used as the experimental material. Plants were grown in an illumination incubator at a temperature of 22°C, with a humidity of 60% and 8/16 h light cycle (8 h light and 16 h dark). *Nicotiana benthamiana* L. (tobacco) were grown in a greenhouse at 22°C and a light cycle of 16/8 h (16 h light and 8 h dark). The UV-B (Philips TL20W/01RS narrowband UV-B tubes) dose was 5 W m^{-2} and irradiated along with the light cycle. The gene-silenced plants were irradiated under the white light or white light plus UV-B for 7 days after infection with Barely Stripe Mosaic Virus (BSMV).

Construction of BSMV-VIGS vectors

The bioinformatics analysis of PCNA was carried out by European Molecular Biology Laboratory–European Bioinformatics Institute (EMBL-EBI; https://www.ebi.ac.uk/) and National Center for Biotechnology Information (NCBI; https://www.ncbi.nlm.nih.gov/). Ligation-independent cloning (LIC) was used to carry out vector attachment, and the LIC cloning site was added on the specific primers (*PCNA*-1-F: AAGGAAGTTTAAATGTTGGAGCTGAGGCTGG, *PCNA*-1-R: AACCACCACCACCGTGGTACTCGGAGTCGGGGA, *PCNA*-2-F: AAGGAAGTTTAATCCGAGTACCAGGCCAT, *PCNA*-2-R: AACCACCACCACCGTTCATGCCTTCATTT CCTCA) for the gene clone (GenBank accession: KM087781.1). By referring to the research of Yuan *et al.* (2011), the specific linking mode and LIC-specific cloning site were obtained. The products were transformed into *E. coli* DH5α after the completion of ligation. The positive colonies were screened based on antibiotic resistance, and colony polymerase chain reaction (PCR) was used for identification.

Agroinfiltration of N. benthamiana *and viral inoculation on wheat*

The *pCaBS*-α, *pCaBS*-β, and *pCa*-γ were transformed into *Agrobacterium* GV3101. Colonies were placed in 10 mL yeast extract broth (YEB) liquid medium with antibiotics and shaken at 200 rpm at 28°C for 10–12 h. The bacteria were collected by 2150*g* centrifugation at OD600 of 1.8. The *Agrobacterium* bacteria were resuspended with suspension buffer (1 M MgCl$_2$.6H$_2$O, 10 mM 2-(N-morpholino) ethanesulfonic acid, 4-morpholineethanesulfonic acid, and 20 μM acetosyringone) at OD600 = ~0.8. The mixture was then injected into four to eight plants of *N. benthamiana* in the leaf stage. After inoculation for 7–12 days, tobacco leaves were ground in the wheat inoculation buffer (phosphate-buffered saline buffer with 1% diatomaceous earth and 0.1% sodium sulfite) for the infection of wheat leaves. Wearing surgical gloves, the forefinger and thumb were dipped into the inoculation buffer and used to rub the wheat leaves sprayed with emery.

Plant height, leaf area, biomass, and chlorophyll content measurements

Plant height was measured with a vernier calliper. Leaf area measurements were performed as described by Schulz *et al.* (2012). Biomass (fresh weight) was detected with an analytical balance. Around 30 leaves were subjected to different treatments, and the results were shown as average values. The extraction and detection of chlorophyll content were conducted using method described by Bruuinsma (1963).

RNA extraction and quantitative reverse-transcription PCR analysis

The total RNA was extracted by the Trizol method. The wheat leaves of each treatment group were strictly quantified at the initial stage of extraction, and the concentration was determined and unified for the synthesis of the first-strand cDNA after extraction. Then, quantitative reverse-transcription PCR was performed by a SuperMix with the following primers: qF: GACTGTTGGTCCATGGATTTTC; qR: ACCAACAGTCAC AGATACAAGT.

Determination of physicochemical and metabolism parameters

After the *TaPCNA* was silenced for 7 days, the wheat leaves were collected for the measurement of physiological parameters. The malondialdehyde (MDA) content was measured by thiobarbituric acid reaction. The superoxide dismutase (SOD) activity was assayed by measuring its capability to inhibit the photochemical reduction of nitroblue tetrazolium. The peroxidase (POD) activity was determined by monitoring the formation of guaiacol dehydrogenation products via following the rise of absorbance at 470 nm over 1 min. The catalase (CAT) activity was determined by monitoring the decomposition of H$_2$O$_2$ at 240 nm (Liu *et al.* 2018). Soluble sugar and soluble protein contents were determined by the anthrone method and Coomassie blue staining, respectively (Zhao *et al.* 2012).

DNA extraction and detection

Total DNA of wheat leaves was extracted by the modified cetyltrimethylammonium bromide (CTAB) method (Abdel-Latif and Osman 2017). Agarose gel was used to detect the integrity of the extracted DNA, and DNA laddering was observed. The gel results were observed by Azure C300 gel imaging system (Azure Ltd).

Propidium iodide (PI) staining

Wheat leaves were cut into squares of 0.5 × 0.5 cm^2, and PI solution with a concentration of 1 μg mL^{-1} was prepared. The leaves were vacuumised in a 1 mL glass syringe for ~15 s, rinsed with water, and observed with an Olympus IX81 fluorescence microscope.

Cell length calculation and data analysis

Figures of the different treatments were obtained during microscopic observation and measured in Image J using the scale bar as a standard. Data results were expressed as means ± s.e. Statistical significance of data was assessed using

one-way analysis of variance tests using the general linear model, and Tukey's test was performed using SPSS 21.0 and Sigma-plot 12.5 to compare the treatment means.

Results

Bioinformatics analysis of TaPCNA

PCNA had a conservative structure domain, whereas the N- and C-terminals presented topological structures during the analysis of protein structure via an online website (Fig. 1). Three PCNA molecules formed a loop close to the DNA double helix. Given the limitation of the carried gene fragments of the virus vector, *PCNA* was divided into two fragments based on the N- and C-terminals considered in this research, and they were named *TaPCNA-1* (400 bp) and *TaPCNA-2* (402 bp), respectively.

Agrobacterium-*mediated BSMV-VIGS in* N. benthamiana *and wheat*

Fig. 2a shows *N. benthamiana* leaves after inoculation with BSMV-VIGS mediated by *Agrobacterium* for 7–15 days. Among the three treatments involving inoculation with virus vectors, BSMV:00 showed symptoms of viral infection. BSMV:*TaPCNA-1* and BSMV:*TaPCNA-2* showed different degrees of leaf edge curling, small leaf areas (Fig. 2b, e), and plant dwarfing

(Figs 2b, 3e). Biomass and chlorophyll content were also examined in each group (Fig. 2f). The injection of BSMV vectors resulted in a reduction in leaf biomass and chlorophyll content in tobacco. In consideration of its evolutionary conservatism, PCNA is similar to a gene-silencing phenotype reported previously (Bruce *et al.* 2011), indicating that *N. benthamiana* was successfully infected with the virus. We inferred that the phenotype changed given that PCNA is a key factor in meristem growth. After *BSMV:TaPCNA* was used to infect the wheat, the overall growth of the plant weakened and dwindled at 13–15 days (Fig. 2c). In addition, wheat leaves showed signs of virus infection (Fig. 2d). We also calculated the leaf area, plant height, biomass, and chlorophyll content in each wheat seedlings under different treatments (Fig. 2g, h). The BSMV vector infestation reduced leaf area, plant height, and biomass in wheat. However, the statistical results showed non-significant differences between PCNA-silenced groups and significant differences with BSMV:00-treated groups (Fig. 2g, h). This finding indicates that PCNA silencing reduced the leaf area, plant height, and biomass. The statistical results on chlorophyll content showed the non-significant difference between BSMV:00 and PCNA silencing group (Fig. 2h). This result indicates that PCNA silencing caused no significant effect on the chlorophyll content of leaf wheat.

Fig. 1. Analysis of TaPCNA protein. (*a*) TaPCNA domain from NCBI blast. PCNA belongs to the PCNA_N superfamily. (*b*) TaPCNA domain structure from EMBL-EBI blast. The results showed N-terminal of TaPCNA comprising 1–125 amino acids, whereas the C-terminal consisted of 127–254 amino acids.
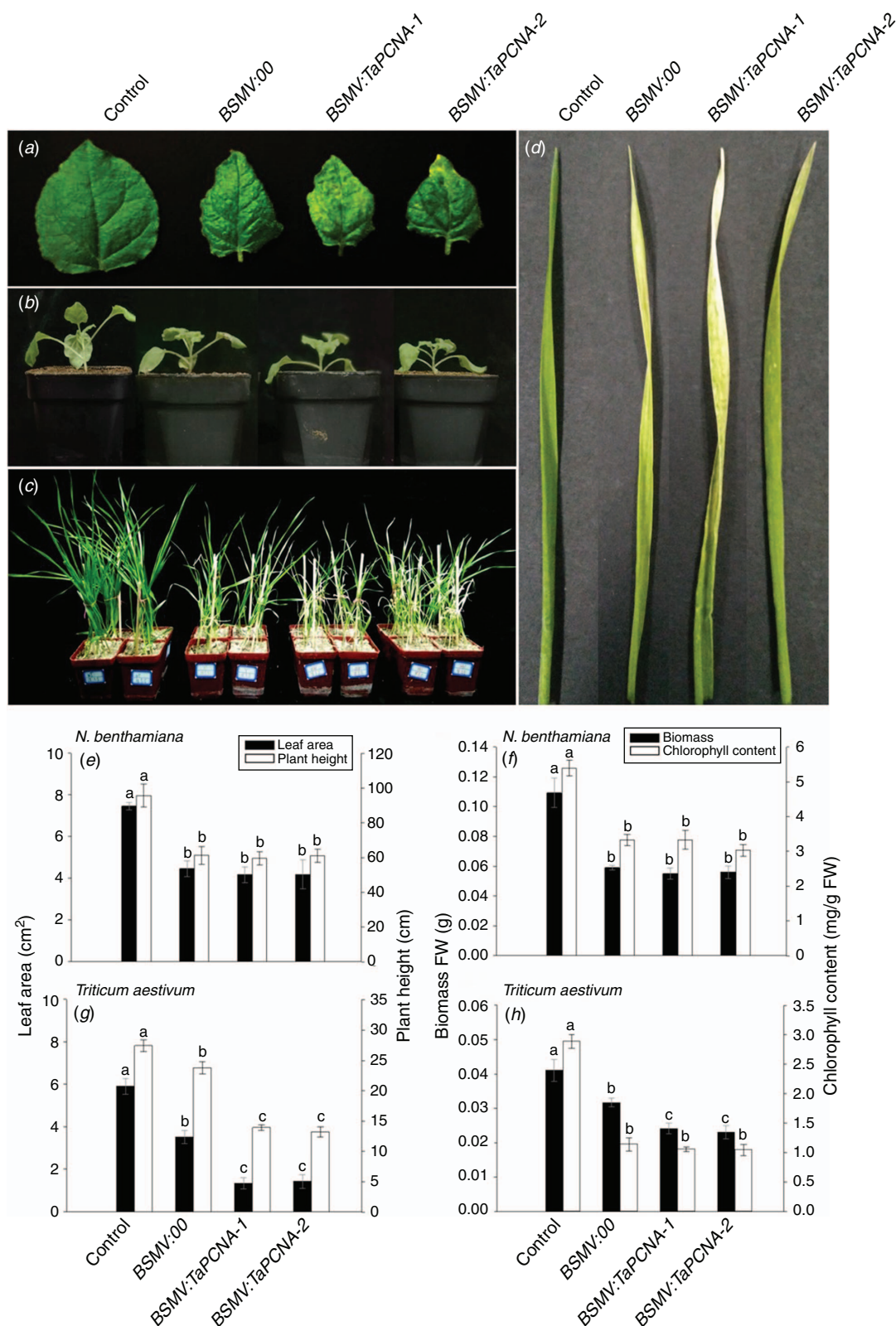
Fig. 2. Infection by BSMV through inoculation into *Nicotiana benthamiana* L. and wheat leaves. (*a*) Phenotype of *N. benthamiana* leaves showed abnormal leaf development. (*b*) Growth of *N. benthamiana* in different treatments. (*c*) Wheat was presented as a dwarf after the *TaPCNA* gene silencing. (*d*) Changes in wheat leaves after virus infection. (*e*) Leaf area and plant height of *N. benthamiana* and wheat (*g*) under different treatments. Biomass and chlorophyll contents of (*f*) *N. benthamiana* and (*h*) wheat in each group. Data are presented as means ± s.e. Means within the same column sharing the same superscript letter do not differ significantly at the 5% level.

The growth rate of gene-silenced plants was statistically calculated (Fig. 3). The 5-day-old wheat seedlings were inoculated, and the calculation began on the 10th day and lasted until the 27th day. The *BSMV*:*TaPCNA-1* and *BSMV*:*TaPCNA-2* groups showed evident growth stagnation on the 15th day of the growth period (at 10 days after inoculation). Meanwhile, the growth rates of the WT (wild type) and *BSMV:00* groups dropped slowly with the extension of growth cycle during the late growth stage. The orange lines indicate the decreasing trends of growth rate in different treatments.

The length of mesophyll cells was recorded and calculated to further test the effect of PCNA silencing on wheat leaf growth (Fig. 4). The cell length of *BSMV:TaPCNA-1* and *BSMV:TaPCNA-2* groups were significantly shorter than that of the WT and *BSMV:00* groups because the latter showed no significant difference.

TaPCNA expression after VIGS and exposure to UV-B

The phenotype of wheat processed with VIGS was maintained for 15–25 days. However, the plants can recover on the 30th day after inoculations. Therefore, the total RNA was extracted from 1, 7 and 22-day-old wheat leaves after gene silencing, and quantitative reverse-transcription PCR was performed to determine the efficiency of VIGS. The expression of *TaPCNA* in *BSMV:TaPCNA-1* and *BSMV*:*TaPCNA-2* groups decreased significantly (Fig. 5a), indicating that *BSMV*::*TaPCNA* interfered with the

expression of *TaPCNA*. To test the response of *TaPCNA* to UV-B, we extracted the total RNA from seedlings after irradiation with UV-B. Compared with the leaves under normal condition (L), the expression level of *TaPCNA* increased in leaves exposed to UV-B (LB) (Fig. 5b). However, the expression was reduced in root under UV-B (RB) after the comparison with root without UV-B exposure (R).

Changes in physiochemical and metabolism parameters of wheat after VIGS and treatment with UV-B

POD is associated with respiration, photosynthesis, and auxin oxidation of plants (De Gara 2004). The activity of POD was measured on the 7th day after *TaPCNA* silencing (Fig. 6a). The activity of POD in *BSM:00* group showed no significant difference from that of the WT group, whereas the activity of POD in *BSMV:TaPCNA-1* and *BSMV:TaPCNA-2* groups decreased compared with those in WT and *BSMV:00* groups. The activity of POD on the 7th day was considerably higher than that on the 1st day after virus infection. These results indicate that the silenced *TaPCNA* affected plant growth and caused a tremendous accumulation of peroxides, affecting the overall plant growth. CAT can remove the excess accumulated H_2O_2 and indirectly reflects the stress resistance and metabolic intensity of plants (Fig. 6b). The activity of CAT in *BSMV:TaPCNA-1* and *BSMV:TaPCNA-2* groups was notably lower compared with that in WT and *BSMV:00* groups.

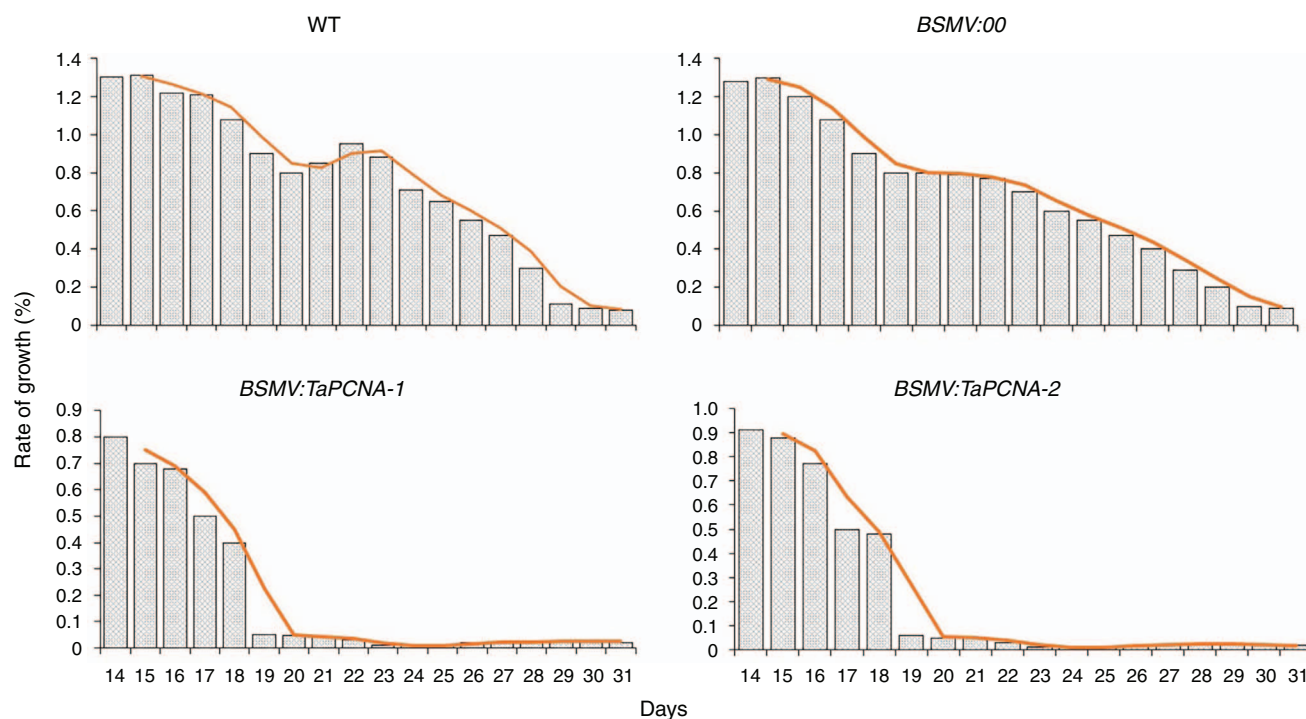The concentration of MDA reflects the degree of lipid peroxidation in the plant cell membrane. The contents of

Fig. 3. Growth rate of different treatments. All treatments showed a decreased growth rate. The WT and *BSMV:00* treatment groups showed a gradual downward trend. Meanwhile, the *BSMV:TaPCNA-1* and *BSMV:TaPCNA-2* groups exhibited a drastic decrease in growth rate after virus infection. The orange line indicates the data trend.
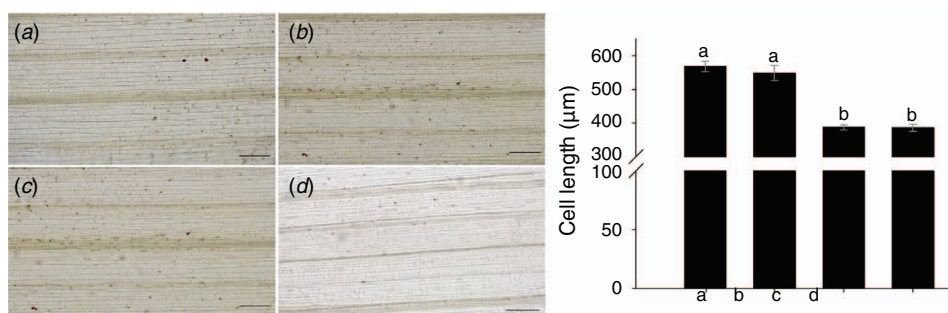
Fig. 4. Mesophyll cell lengths of (*a*) WT, (*b*) *BSMV*:*00*, (*c*) *BSMV*:*TaPCNA-1* and (*d*) *BSMV*:*TaPCNA-2* groups. The histogram shows the calculated cell length. Bar, 50 μm. Data are presented as means ± s.e. Means within the same column sharing the same superscript letter do not differ significantly at the 5% level.
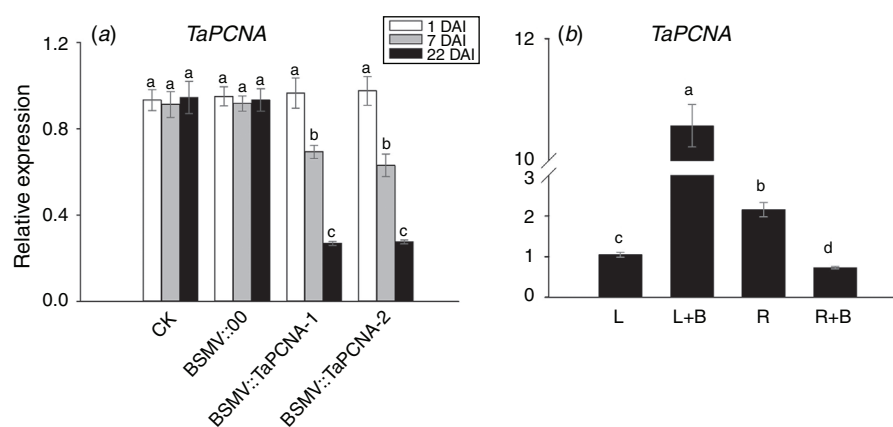

Fig. 5. Expression level of *TaPCNA* in different treatments determined by quantitative reverse-transcription PCR. (*a*) *TaPCNA* expression pattern in different groups on 1, 7, and 22 days after infection. (*b*) Expression level of *TaPCNA* in different groups. L, LB, R, and RB indicate the leaves, leaves under UV-B, root and root exposure to UV-B radiation. Data are presented as means ± s.e. Means within the same column sharing the same superscript letter do not differ significantly at the 5% level.

MDA in *BSMV*:*TaPCNA-1* and *BSMV*:*TaPCNA-2* groups increased compared with those in WT and *BSMV*::*00* groups (Fig. 6*c*). In addition, MDA is a substance product of membrane lipid under the action of reactive oxygen species, indicating that the membrane was damaged after the silencing of *TaPCNA*. SOD removes free oxygen radicals in cells. The activity of SOD in *BSMV*:*TaPCNA-1* and *BSMV*:*TaPCNA-2* groups decreased compared with those in WT and *BSMV*::*00* groups (Fig. 6*d*). After the treatment with UV-B, the activities of POD and CAT decreased, whereas the SOD activity and MDA content increased in each treatment group. Moreover, WT+B, *BSMV*:*TaPCNA-1*+B, and *BSMV*:*TaPCNA-2*+B groups showed the same trend.

Soluble sugar and soluble protein contents are useful parameters reflecting the metabolic process of plants. After constructing the standard curve (Fig. 6*e, g*), we calculated the contents of soluble sugar and soluble protein. Total contents of soluble sugar and soluble protein in *BSMV*:*TaPCNA-1* and *BSMV*:*TaPCNA-2* groups decreased remarkably compared with those in WT and *BSMV*:*00* groups (Fig. 6*f, h*). These results indicate that the metabolism of plants was slowed

down. The findings also indirectly prove that the silencing of *TaPCNA* affected plant growth, especially after being exposed to UV-B.

PCD in wheat leaves after VIGS and exposure to UV-B

The DNA of wheat plants in *TaPCNA*-silenced groups was extracted. Gel electrophoresis showed the complete DNA bands of WT and *BSMV*:*00* groups, whereas the DNA of *BSMV*:*TaPCNA-1* and *BSMV*:*TaPCNA-2* were dispersed as DNA laddering (Fig. 7). The WT+B and *BSMV*:*00*+B groups showed regular low-molecular-weight fragments and similar fragmentation and dispersion with *BSMV*:*TaPCNA-1*+B and *BSMV*:*TaPCNA-2*+B groups, indicating the occurrence of DNA damage and PCD in wheat cells.

PI staining was carried out on the wheat leaves in different groups to confirm the PCD of wheat cells after *TaPCNA* silencing. As shown in Fig. 8, the dead cells showed an evident contour. The view of WT and *BSMV*:*00* groups was dark and heavy, whereas the *BSMV*:*TaPCNA-1* and *BSMV*: *TaPCNA-2* groups (Fig. 8*a*) exhibited more shiny and coloured
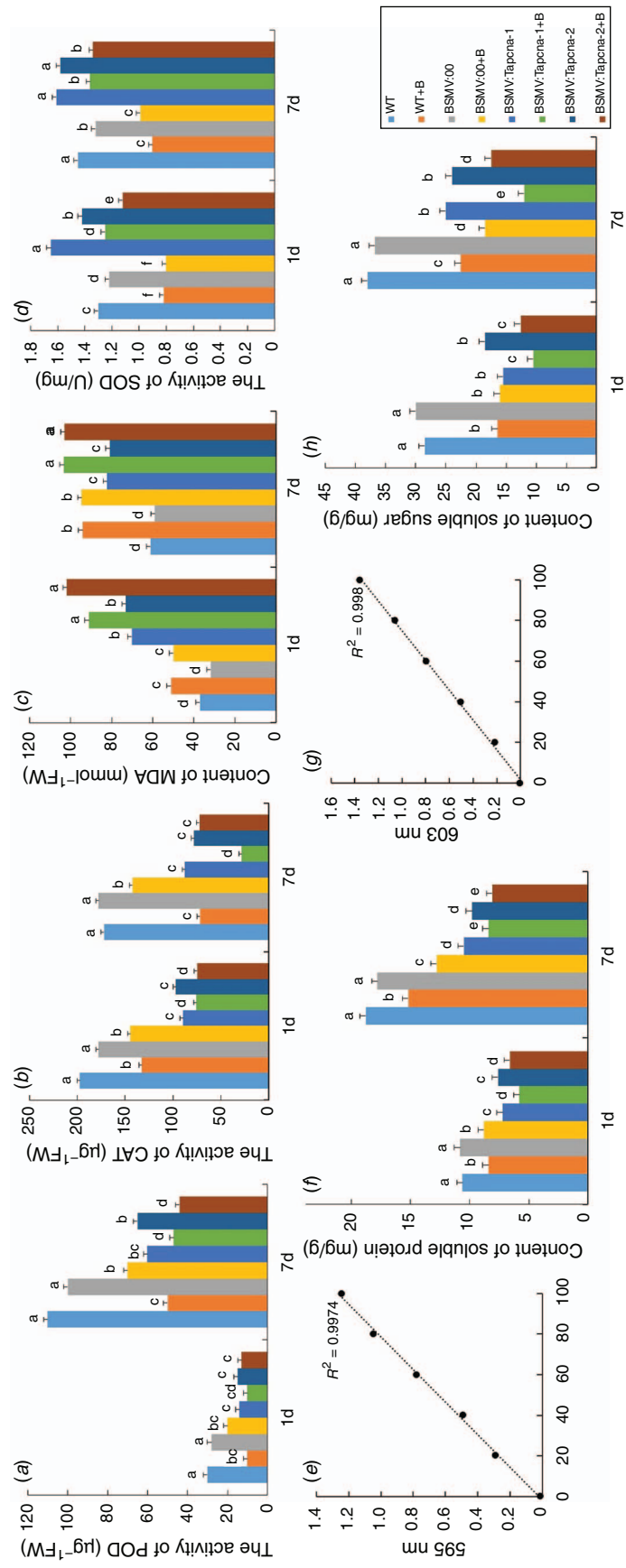
Fig. 6. Determination of physicochemical and metabolism parameters. (*a*) POD activity in different groups. (*b*) CAT activity in different groups. (*c*) MDA content in different groups. (*d*) SOD activity in different groups. (*e*) Standard protein curve. (*f*) Soluble protein content in different groups. (*g*) Standard sucrose curve. (*h*) Soluble sugar content. Data are means ± s.e., and values followed by various letters are significantly different (*P* < 0.05).

parts. After magnification, normal cells showed a clear red notch, as seen in parts (i) and (ii) of Fig. 8*b*. The cell nucleus obtained after PCD can be stained in red, as seen in parts (iii) and (iv) of Fig. 8*b*. The results indicated the inhibition of wheat growth caused by *TaPCNA* silencing-induced PCD. PI staining was also carried out for each treatment group after UV-B treatment. As shown in Fig. 8*a*, all groups can be observed and exhibited different degrees of red-coloured parts after the treatment with UV-B. Meanwhile, the *BSMV*:*TaPCNA-1*+B

and *BSMV*:*TaPCNA-2*+B groups showed more coloured parts than the WT+B and *BSMV*:*00*+B groups.

Discussion

In this paper, TaPCNA presented important functions consistent with the findings of previous studies, including DNA damage repair and other processes in the whole lifecycle (Leung *et al*. 2019). Previous studies reported that the structure of PCNA is made up of three molecules to form a closed-loop structure, and both ends of the topological structure are similar (Ripley *et al*. 2020). Here, phenotypic analysis revealed that the *PCNA*-silenced plants were shorter than the WT and *BSMV*:*00* groups (Fig. 2). Statistics and calculations of the growth rate revealed that the plants had significantly stagnated growth after gene silencing (Figs 2, 3). For further verification, the results of cell size showed that the gene silencing group was shorter than the WT and *BSMV*: *00* groups (Fig. 4). Thus, PCNA affects the growth of meristem of wheat leaves.

Subsequently, to investigate the importance of *PCNA* in the plant growth cycle, we tested the activity of several key enzymes in the antioxidant system (Fig. 6). The results showed that *PCNA* gene silencing affected the physiological metabolism of wheat and weakened the resistance of wheat. The contents of soluble sugar and soluble protein that reflect the intensity of metabolism were measured, and the contents of two substances decreased. This result reflects that plant metabolism slows down after *PCNA* silencing, and growth may be blocked or stopped. These results suggest that after *PCNA* gene silencing, DNA replication is blocked and affects
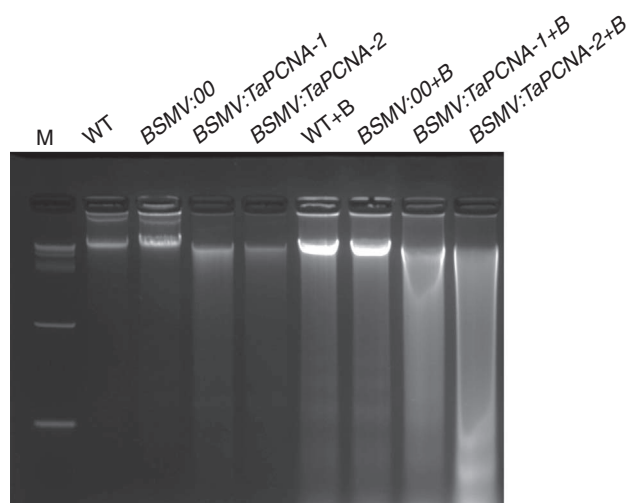

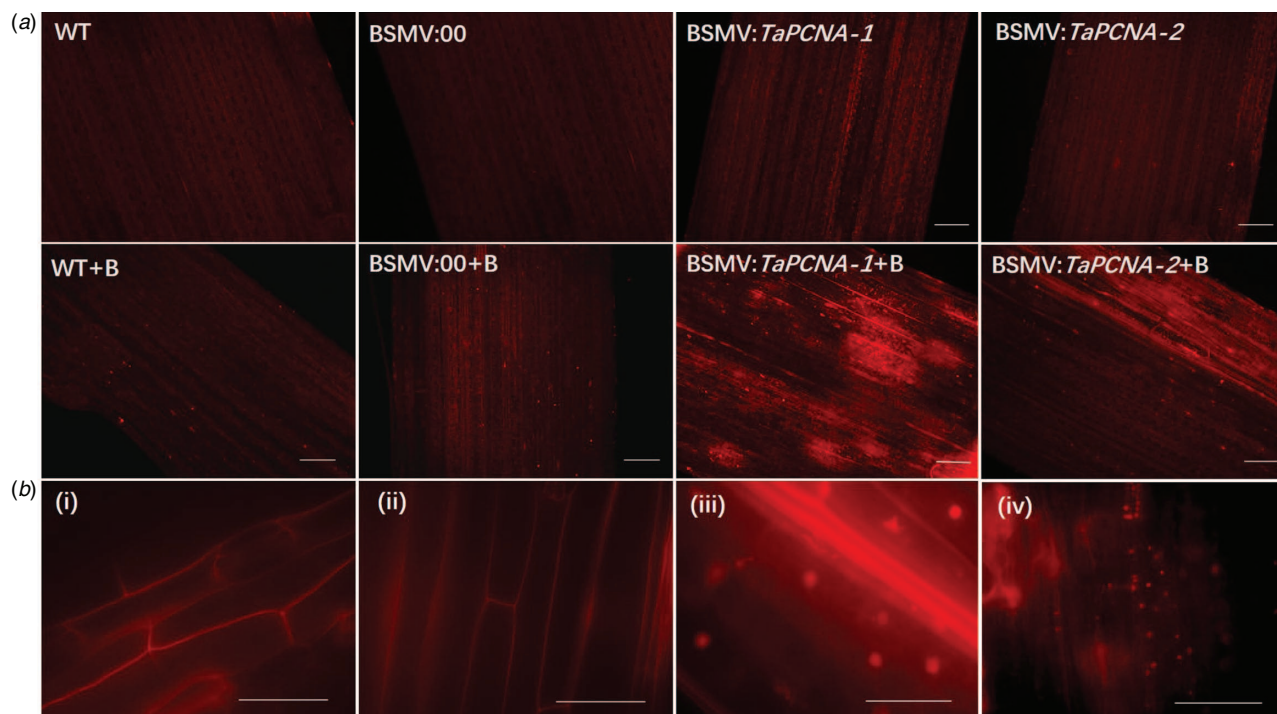**Fig. 7.** DNA laddering in different treatments.

Fig. 8. Results of PI staining in each group. (*a*) Different treatment groups after PI staining. (*b*) Parts (i) and (ii) represent for normal cell staining, parts (iii) and (iv) represent for PCD cell nuclear staining. Bar, 50 μm.

chromatin synthesis, which leads to cycle block and several instances of PCD (Qian *et al*. 2019). The DNA laddering results showed the diffused DNA of plants after *PCNA* gene silencing (Fig. 7). Therefore, after DNA damage, PCNA becomes involved in certain damage repair processes. For specific cells that cannot be repaired, such condition may eventually lead to PCD.

To further verify the PCD phenomenon, we attempted to advance the effective period of gene silencing to the seedling stage through a series of other inoculation methods, such as vacuum inoculation of immature embryos, tobacco-leaf liquid soaking, hydroponic inoculation, and *Agrobacterium* suspension soaking in the early stage of this study. However, the limitation of BSMV-VIGS technology cannot be achieved. Therefore, the phenomenon of PCD can only be observed in the seedling stage. The results of PI staining showed bright areas in the visual field of the *PCNA* gene-silencing group, suggesting the occurrence of PCD (Fig. 8). These findings may be important reasons for the changes in wheat physiological metabolism. In previous studies, the effect of PCNA on plant physiological metabolism was generally disregarded. Although several key physiological processes involved in PCNA have been ignored, more attention to this aspect is needed in the future. VIGS is a powerful and reliable tool to investigate gene functions and disease research in numerous crop plants (Li *et al*. 2020). Meanwhile, in other studies on gene functions, VIGS was not considered the best method because it can be used in certain transgenic plants but not all stages of the life cycle. In later research, we can explore convenient inoculation techniques that can be applied in the early stage of plants to expand the use period of this technology and extend it to a larger scale. Finally, we also explore more gene-editing techniques for wheat to study gene functions and provide a theoretical basis to improve wheat agronomic traits.

Although wheat PCNA has been reported sparingly, our results suggest that it is essential and is involved in the normal growth and affects the occurrence of DNA damage and PCD. Given that UV-B is an intrinsic component of sunlight, our study can provide experimental evidence for studying the effects of light on crops and provide a theoretical basis for further modification of crop traits.

Conflicts of interest

The authors declare no conflict of interest.

Declaration of funding

References

Abdel-Latif A, Osman G (2017) Comparison of three genomic DNA extraction methods to obtain high DNA quality from maize. *Plant Methods* **13**(1), 1–9. doi:10.1186/s13007-016-0152-4

Bruce G, Gu M, Shi N, Liu Y, Hong Y (2011) Influence of retinoblastoma-related gene silencing on the initiation of DNA replication by African cassava mosaic virus Rep in cells of mature leaves in *Nicotiana benthamiana* plants. *Virology Journal* **8**, 561. doi:10.1186/1743-422X-8-561

Bruuinsma J (1963) The quantitative analysis of chlorophylls a and b in plant extracts. *Photochemistry and Photobiology* **2**, 241–249. doi:10.1111/j.1751-1097.1963.tb08220.x

Chen K, Gao C (2015) Targeted gene mutation in plants. In 'Somatic Genome Manipulation'. Eds Li, Xiu-Qing, Donnelly, Danielle J., Jensen, Thomas G. pp. 253–272. (Springer)

De Gara L (2004) Class III peroxidases and ascorbate metabolism in plants. *Phytochemistry Reviews* **3**, 195–205. doi:10.1023/B:PHYT.00000 47795.82713.99

Essers J, Theil AF, Baldeyron C, van Cappellen WA, Houtsmuller AB, Kanaar R, Vermeulen W (2005) Nuclear dynamics of PCNA in DNA replication and repair. *Molecular and Cellular Biology* **25**, 9350–9359. doi:10.1128/MCB.25.21.9350-9359.2005

Hopkins L, Bond M, Tobin A (2002) Ultraviolet-B radiation reduces the rates of cell division and elongation in the primary leaf of wheat (*Triticum aestivum* L. cv Maris Huntsman). *Plant, Cell & Environment* **25**, 617–624. doi:10.1046/j.1365-3040.2002.00834.x

Kelman Z (1997) PCNA: structure, functions and interactions. *Oncogene* **14**, 629–640. doi:10.1038/sj.onc.1200886

Kuhlmann F, Müller C (2010) UV-B impact on aphid performance mediated by plant quality and plant changes induced by aphids. *Plant Biology* **12**, 676–684. doi:10.1111/j.1438-8677.2009.00257.x

Leung W, Baxley RM, Moldovan G-L, Bielinsky A-K (2018) Mechanisms of DNA damage tolerance: Post-translational regulation of PCNA. *Genes* **10**(1), 10. doi:10.3390/genes10010010

Li Y, Liu Y, Qi F, Deng C, Lu C, Huang H, Dai S (2020) Establishment of virus-induced gene silencing system and functional analysis of *ScbHLH17* in *Senecio cruentus*. *Plant Physiology and Biochemistry* **147**, 272–279. doi:10.1016/j.plaphy.2019.12.024

Liu W, Xu F, Lv T, Zhou W, Chen Y, Jin C, Lu L, Lin X (2018) Spatial responses of antioxidative system to aluminum stress in roots of wheat (*Triticum aestivum* L.) plants. *The Science of the Total Environment* **627**, 462–469. doi:10.1016/j.scitotenv.2018.01.021

Lizana XC, Hess S, Calderini DF (2009) Crop phenology modifies wheat responses to increased UV-B radiation. *Agricultural and Forest Meteorology* **149**, 1964–1974. doi:10.1016/j.agrformet.2009.07.003

Maga G, Hübscher U (2003) Proliferating cell nuclear antigen (PCNA): a dancer with many partners. *Journal of Cell Science* **116**, 3051–3060. doi:10.1242/jcs.00653

Mailand N, Gibbs-Seymour I, Bekker-Jensen S (2013) Regulation of PCNA–protein interactions for genome stability. *Nature Reviews. Molecular Cell Biology* **14**, 269–282. doi:10.1038/nrm3562

Nawkar GM, Maibam P, Park JH, Sahi VP, Lee SY, Kang CH (2013) UV-Induced cell death in plants. *International Journal of Molecular Sciences* **14**, 1608–1628. doi:10.3390/ijms14011608

Paunesku T, Mittal S, Protić M, Oryhon J, Korolev S, Joachimiak A, Woloschak G (2001) Proliferating cell nuclear antigen (PCNA): ringmaster of the genome. *International Journal of Radiation Biology* **77**, 1007–1021. doi:10.1080/09553000110069335

Qian J, Chen Y, Xu Y, Zhang X, Kang Z, Jiao J, Zhao J (2019) Interactional similarities and differences in the protein complex of PCNA and DNA replication factor C between rice and *Arabidopsis*. *BMC Plant Biology* **19**, 257. doi:10.1186/s12870-019-1874-z

Ries G, Heller W, Puchta H, Sandermann H, Seidlitz HK, Hohn B (2000) Elevated UV-B radiation reduces genome stability in plants. *Nature* **406**, 98–101. doi:10.1038/35017595

Ripley BM, Gildenberg MS, Washington MT (2020) Control of DNA damage bypass by ubiquitylation of PCNA. *Genes* **11**(2), 138. doi:10.3390/genes11020138

Schulz P, Neukermans J, Van Der Kelen K, Mühlenbock P, Van Breusegem F, Noctor G , et al. (2012) Chemical PARP inhibition enhances growth of *Arabidopsis* and reduces anthocyanin accumulation and the activation of stress protective mechanisms. *PLoS One* **7**, e37287. doi:10.1371/journal.pone.0037287

Shewry PR (2009) Wheat. *Journal of Experimental Botany* **60**, 1537–1553. doi:10.1093/jxb/erp058

Strzalka W, Ziemienowicz A (2011) Proliferating cell nuclear antigen (PCNA): a key factor in DNA replication and cell cycle regulation. *Annals of Botany* **107**, 1127–1140. doi:10.1093/aob/mcq243

Yin R, Ulm R (2017) How plants cope with UV-B: from perception to response. *Current Opinion in Plant Biology* **37**, 42–48. doi:10.1016/j.pbi.2017.03.013

Yuan C, Li C, Yan L, Jackson AO, Liu Z, Han C, Yu J, Li D (2011) A high throughput barley stripe mosaic virus vector for virus induced gene silencing in monocots and dicots. *PLoS One* **6**(10), e26468. doi:10.1371/journal.pone.0026468

Zhao S, Huang Q, Yang P, Zhang J, Jia H, Jiao Z (2012) Effects of ion beams pretreatment on damage of UV-B radiation on seedlings of winter wheat (*Triticum aestivum* L.). *Applied Biochemistry and Biotechnology* **168**, 2123–2135. doi:10.1007/s12010-012-9922-2

Handling Editor: Vadim Demidchik